Chin. Geogra. Sci. 2016 Vol. 26 No. 6 pp. 731–744
doi: 10.1007/s11769-016-0833-y

Springer Science Press
www.springerlink.com/content/1002-0063

Evaluation of Spectral Scale Effects in Estimation of Vegetation Leaf Area Index Using Spectral Indices Methods

DU Huishi[1, 2], JIANG Hailing[2], ZHANG Lifu[3], MAO Dehua[1] ,WANG Zongming[1]

(1. *Northeast Institute of Geography and Agroecology*, *Chinese Academy of Sciences*, *Changchun* 130102, *China*; 2. *College of Tourism and Geographical Science*, *Jilin Normal University*, *Siping* 136000, *China*; 3. *Institute of Remote Sensing and Digital Earth*, *Chinese Academy of Sciences*, *Beijing* 100101, *China*)

Abstract: Spectral index methodology has been widely used in Leaf Area Index (LAI) retrieval at different spatial scales. There are differences in the spectral response of different remote sensors and thus spectral scale effect generated during the use of spectral indices to retrieve LAI. In this study, PROSPECT, leaf optical properties model and Scattering by Arbitrarily Inclined Layers (SAIL) model, were used to simulate canopy spectral reflectance with a bandwidth of 5 nm and a Gaussian spectral response function was employed to simulate the spectral data at six bandwidths ranging from 10 to 35 nm. Additionally, for bandwidths from 5 to 35 nm, the correlation between the spectral index and LAI, and the sensitivities of the spectral index to changes in LAI and bandwidth were analyzed. Finally, the reflectance data at six bandwidths ranging from 40 to 65 nm were used to verify the spectral scale effect generated during the use of the spectral index to retrieve LAI. Results indicate that Vegetation Index of the Universal Pattern Decomposition (VIUPD) had the highest accuracy during LAI retrieval. Followed by Normalized Difference Vegetation Index (NDVI), Modified Simple Ratio Indices (MSRI) and Triangle Vegetation Index (TVI), although the coefficient of determination R^2 was higher than 0.96, the retrieved LAI values were less than the actual value and thus lacked validity. Other spectral indices were significantly affected by the spectral scale effect with poor retrieval results. In this study, VIUPD, which exhibited a relatively good correlation and sensitivity to LAI, was less affected by the spectral scale effect and had a relatively good retrieval capability. This conclusion supports a purported feature independent of the sensor of this model and also confirms the great potential of VIUPD for retrieval of physicochemical parameters of vegetation using multi-source remote sensing data.

Keywords: spectral index; vegetation leaf area index; radiative transfer model; spectral response; scale effect

Citation: Du Huishi, Jiang Hailing, Zhang Lifu, Mao Dehua, Wang Zongming, 2016. Evaluation of spectral scale effects in estimation of vegetation leaf area index using spectral indices methods. *Chinese Geographical Science*, 26(6): 731–744. doi: 10.1007/s11769-016-0833-y

1 Introduction

Remote sensing provides valuable information for estimation of various agronomic parameters in precision agriculture and can perform field-scale monitoring without destructive sampling of a crop. In particular, spectral reflectance from narrow bands of vegetation leaves and canopies based on multispectral and hyperspectral sensors has been found to be promising for estimation of a large variety of eco-physiological parameters including vegetation light use efficiency (LUE), leaf water content and leaf area index (LAI) (Bicheron and Leroy, 1999; Darvishzadeh *et al*., 2008a; Rogers *et al.*, 2015). LAI, which is defined as one half of the leaf surface area per unit ground surface area, can be used to measure crops and estimate net primary production

Received date: 2016-05-05; accepted date: 2016-09-01
Foundation item: Under the auspices of National Natural Science Foundation of China (No.41401002), Jilin Province Science Foundation for Youths (No. 20160520077JH)
Corresponding author: WANG Zongming. E-mail: zongmingwang@iga.ac.cn

(NPP) (Paul and Edward, 1983; Darvishzadeh *et al*., 2008b). Many studies have shown that timely and accurately measuring crop LAI using remote sensing can be an important tool in understanding plant growth, estimating yield and monitoring crop pests (Goel and Thompson, 1984).

There are typically two methods used for estimating vegetation LAI, which are the experience/semi-empirical method and the radiative transfer model method (Weiss *et al*., 2004). However, the latter method is often restricted in practical applications because it involves complex algorithms and there are difficulties in acquisition of input parameters (Haboudane *et al*., 2002). In contrast, spectral indices based on the experience/semi-empirical method have been widely used due to its simplicity and ability for quick retrieval (Houborg *et al*., 2007). Spectral indices (SIs) have been developed as the algebraic combination using two or more bands of multispectral or hyperspectral bands which are designed to highlight a particular property of vegetation (Bannari *et al*., 1995; Broge and Leblanc, 2001). Therefore, a number of studies have investigated spectral indices that have high sensitivity to LAI in order to estimate crop LAI. The relationship between spectral reflectance and vegetation LAI is often modeled through the use of spectral indices (Daughtry *et al*., 2000; Everitt and Yang, 2007).

Elvidge and Chen (1995) calculated SIs as linear combinations of near infrared (NIR) and visible red reflectance and found them to be well correlated with canopy structure, LAI, and absorbed photosynthetic active radiation (APAR) (Elvidge and Chen, 1995). Broge and Leblanc (2001) compared the prediction power and stability of broadband and hyperspectral SIs for estimation of LAI and canopy density (Broge and Leblanc, 2001). Pisek and Chen (2007) pointed out that various SIs derived from broadband sensors were used due to their ability to retrieve biochemical parameters of vegetation, including LAI and chlorophyll content (Pisek and Chen, 2007). Wu *et al.* (2010a; 2010b) established spectral indices that incorporated red edge wavelengths of 705 nm and 750 nm to estimate LAI of wheat reliably.

Many studies have focused on optimal band selection and spectral indices composition in order to improve prediction accuracy, but have ignored the effect of spectral scale of spectral indices caused by spectral response features of particular sensors. Identical spectral indices derived from diverse sensors will exhibit different prediction accuracy and stability during estimation of vegetation LAI (Moody and Woodcock, 1995; Marceau and Hay, 1999). Scholar pointed out that, due to the complexity of ground objects on land surfaces, methods developed at one scale may not be applicable at another scale (Su *et al*., 2001; Wen *et al*., 2009). For a given object of study (such as vegetation), when spectral data with different spectral resolutions (spectral scales) are used to study the accuracy of the retrieval of physicochemical parameters by spectral indices, retrieval results are usually significantly different due to the presence of differences in the spectral response, the center wavelength and the full width at half maximum (FWHM). Therefore, during the retrieval of vegetation physicochemical parameters, it is necessary to study the retrieval capacity and accuracy of spectral index models at different spectral scales.

The research of spectrum scale was minority. In some relevant studies, ′spectrum scale′ also be called ′spectrum effect′. The response intensity and bandwidth of bands from different sensor to surface feature had differences, appeared in different spectral response value and FWHM. Therefore, there are great difference among vegetation canopy information in various band position and band width. Selection of optimal band was the basis of structure of spectral index, establishment of experience model of spectrum parameters, and sensor band settlement. Cho (2006) put forward linear extrapolation method to determine red edge position, in order to successfully estimate nitrogen content of rye and corn (Cho and Skidmore, 2006). Darvishzadeh *et al*. (2008b) used Spectra Vista Corporation (SVC) GER 3700 spectra data, which between 400 nm and 2400 nm including 584 bands, constructed all possible spectrum indices, and then established correlation between spectral indices and LAI, leaf chlorophyll content of grass, and ultimately determined the optimal band position (Darvishzadeh *et al*., 2008a). Most research about effect of band width on vegetation parameters estimation concentrated in inferiority of multispectral and hyperspectral indices and, as well as the optimal band width selection. Thenkabail (2002) used six kinds of crops to analysis correlation between spectral indices and vegetation parameters, such as LAI, nitrogen content, in order to determine the 12 core spectral bands and the corresponding optimal spectral index (Thenkabail *et al*., 2000). Teillet

(1997) used Airborne Visible Infrared Imaging Spectrometer (AVIRIS) hyperspectral data to study the influence of forest canopy NDVI by band position and band width, finally draw a conclusion that the red band has a significant impact on index NDVI. When the band width is less than 50 nm, the spectral index value in near infrared wave band was hardly affected by band location (Teillet *et al*., 1997). In a word, the settlement of band position and band width would exerted a significant influence on estimation of vegetation LAI, leaf chlorophyll, nitrogen content and so on.

The aim of this study was to investigate the influence of spectral scale on LAI retrieval using seven typical SIs and to evaluate the performance of Vegetation Index of the Universal Pattern Decomposition (VIUPD) during the estimation of vegetation LAI using multiple spectral scale data.

2 Materials and Method

2.1 Data acquisition and processing

Since it is difficult to obtain synchronous spectral data with multiple bandwidths, vegetation canopy reflectance data with a bandwidth of 5 nm at 0.01, 0.10, 0.25, 0.50, 0.75, 1.00, 1.50, 2.00, 3.00 and 7.00 LAI levels generated from a coupled PROSPECT-SAIL (PROSAIL) model were used as the reference in this study. A Gaussian spectral response function was employed to simulate the reflectance data to the spectral data at bandwidths of 10 nm, 15 nm, 20 nm, 25 nm, 30 nm and 35 nm, in order to study the effect of bandwidth on LAI retrieval using spectral indices. In section 4.2 of this paper, the same method was applied to 40–65 nm bandwidth data for the validation of the spectral scale effect generated during LAI retrieval.

2.1.1 PROSAIL model

The RPOSAIL model was obtained by coupling the PROSPECT leaf model with the Scattering by Arbitrary Inclined Leaves (SAIL) canopy model (Jacquemoud and Baret, 1990). The input parameters of the model included leaf structural parameters (e.g., chlorophyll content, mesophyll structural parameters, leaf equivalent water thickness, and dry matter concentration), canopy structural parameters (e.g., LAI and average leaf inclination angle) as well as the solar elevation angle and azimuth angle of observation. Reflectance and transmittance of the blade were the output parameters of the blade model as well as the input parameters for the canopy model, which can be used to couple the PROSPECT leaf model with the SAIL canopy model, thus correlating vegetation canopy reflectance with vegetation biochemical parameters (Jacquemoud *et al.*, 1995; Feret *et al.*, 2008). For the reflectance information of the model soil, the measured spectral information in the study area or the empirical data in the spectral library could be used, so that the simulated canopy reflectance data were more consistent with actual conditions in the study area. Visibility information could be set according to weather conditions at the time that a geosynchronous satellite had passed over the study area. The settings of the sun angle (zenith, azimuth) and the viewing angle (zenith, azimuth) were similar to that of visibility, and these parameters can adequately describe the state of the solar radiation (Stéphane *et al.*, 2009).

2.1.2 Simulation of canopy reflectance data

The input parameters of the PROSPECT leaf model were set, with the measured data or empirical data used as a reference and the input parameters shown in Table 1. Through model simulation, the blade reflectance and transmittance data in the spectral range of 400–2400 nm were obtained with a spectral sampling interval of 5 nm.

The parameters of the SAIL canopy model were set, and the reflectance and transmittance data obtained from the PROSPECT model were used as the input parameters for the SAIL model. To study the effect of LAI on leaf reflectance, the other input parameters were fixed in the SAIL model, and the values were selected using the measured and empirical data as reference data. The LAI values were chose as 0.01, 0.10, 0.25, 0.50, 0.75, 1.00, 1.50, 2.00, 3.00, and 7.00, as the range from 0.01 to 7.00 covered changes in the LAI values of vegetation throughout the growth cycle. Other input parameters are shown in Table 2.

Table 1 Input parameter settings for PROSPECT leaf model

Parameter	Value	Note
N	1.350	Mesophyll structural parameter
C_{a+b} (μg/cm^2)	40	Concentration of chlorophyll a and chlorophyll b
EWT (g/cm^2)	0.012	Leaf equivalent water thickness
D_m (g/cm^2)	0.010	Dry matter concentration

Table 2 Input parameter settings for SAIL canopy model

Input parameter	Value description
Fraction direct solar	1: all are direct sunlight; 0: all are scattered light in sky
Solar declination	From –23.5 in winter to 23.5 in summer
Latitude (decimal degree)	Used to calculate solar zenith angle
View azimuth angle	When direction of sun is the same as that of observation, value is 0°; when direction of sun is opposite to that of observation, value is 180°
View zenith angle	
Time of day (decimal hour)	Used to calculate solar zenith angle
APAR	Calculate it or not

Note: APAR is absorbed photosynthetic active radiation

The vegetation canopy reflectance data were simulated based on the PROSPECT radiative transfer model and the SAIL canopy model, and the simulation process is shown in Fig. 1.

Based on the coupling of the PROSPECT leaf model and the SAIL canopy model, the simulated canopy reflectance data in the spectral range of 400–2400 nm were obtained with a spectral sampling interval of 5 nm. Figure 2 presents the vegetation canopy reflectance curve in the spectral range of 400–2400 nm under ten LAI levels.

2.1.3 Simulation of multiband spectral data

In order to study the impact of different bandwidths on the retrieval of chlorophyll content in plant leaves, the continuous 5 nm hyperspectral data from the PROSPECT model were simulated to the leaf reflectance data at bandwidths of 10 nm, 15 nm, 20 nm, 25 nm, 30 nm and 35 nm using formulas (1) and (2). Subsequently, the selected spectral indices were calculated based on the reflectance data of these seven bandwidths.

$$\rho_j = \int_{\lambda_s(j)}^{\lambda_e(j)} \rho(\lambda) S_j(\lambda) \mathrm{d}\lambda \Big/ \int_{\lambda_s(j)}^{\lambda_e(j)} S_j(\lambda) \mathrm{d}\lambda \tag{1}$$

where ρ_j is the simulated leaf reflectance for band j, $\rho(\lambda)$ is the simulated 5 nm spectral data from the PROSPECT model, and $\lambda_s(j)$ and $\lambda_e(j)$ are the starting wavelength and ending wavelengths, respectively. $S_j(\lambda)$ is the spectral response function of the corresponding band j. A Gaussian spectral response function was selected in this study and the formula show as follow:

$$S_j(\lambda) = \exp - \left(\frac{\lambda - c_j}{FWHM_k \Big/ \left(2\sqrt{\ln 2}\right)} \right)^2 \tag{2}$$

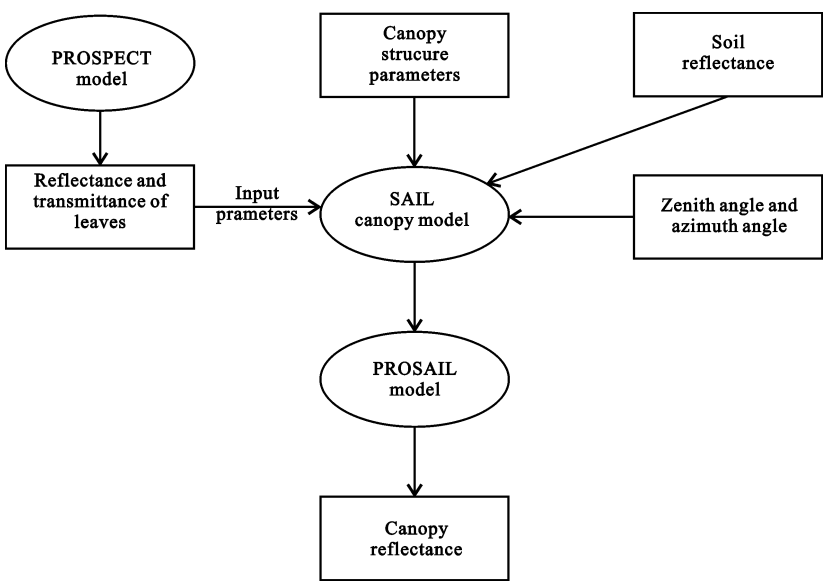

Fig. 1 Flowchart for simulation of canopy reflectance using coupled leaf canopy model

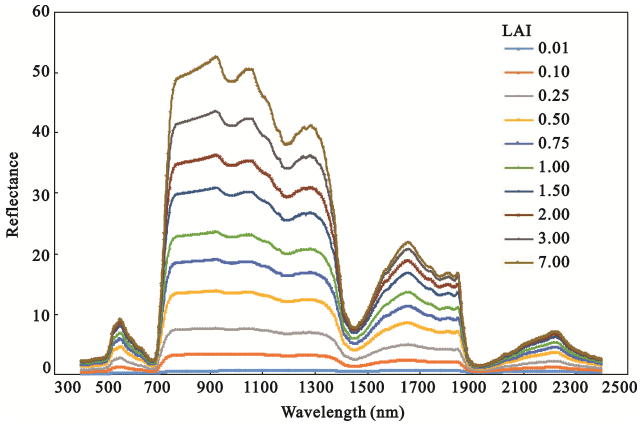

Fig. 2 Canopy reflectance curves at different LAI levels in spectral range of 400–2400 nm

where c_j is the center wavelength of the band j; *FWHM* is the simulated bandwidth, i.e., 10 nm, 15 nm, 20 nm, 25 nm, 30 nm or 35 nm.

2.2 Methods

2.2.1 Selection and calculation of spectral index

A new vegetation index, based on the VIUPD method, derived from the universal pattern decomposition method (UPDM), was also used. In order to acquire more detailed information for vegetation change, a supplementary pattern of yellow-leaf was added into the UPDM (Zhang *et al.*, 2006; Zhang *et al.*, 2007). Therefore the reflectance data of every pixel obtained from different kinds of sensors was decomposed into four spectral patterns of water, vegetation, soil and yellow-leaf as follows:

$$R_i \rightarrow C_w \cdot P_w(i) + \mathrm{C}_v \cdot P_v(i) + \mathrm{C}_s \cdot P_s(i) + \mathrm{C}_4 \cdot P_4(i) \quad (3)$$

where R_i is the reflectance data of band i measured by the ground spectroradiometer, aircraft or satellite sensor for any samples, C_w, C_v, C_s and C_4 are the decomposition coefficients, and $P_w(i)$, $P_v(i)$, $P_s(i)$ and $P_4(i)$ are the standard spectral patterns of pure water, vegetation, soil and yellow-leaf for band i. $P_k(i)$ (k = w, v, s, 4), the four kinds of standard spectral patterns, is defined by

$$P_k(i) = \frac{\int_{\lambda_s(i)}^{\lambda_e(i)} P_k(\lambda)\mathrm{d}\lambda}{\int_{\lambda_s(i)}^{\lambda_e(i)} \mathrm{d}\lambda} (k = w, v, s, 4) \quad (4)$$

where $\lambda_s(i)$ and $\lambda_e(i)$ represent the starting and ending wavelength of band i respectively, and $P_k(\lambda)$ is the stand spectral pattern of continuous wavelength λ. The VIUPD expressed as a linear sum of the pattern decomposition coefficients (Zhang *et al.*, 2003; Zhang *et al.*, 2010) was calculated as

$$VIUPD = \frac{(C_v - 0.1 \times C_s - C_4)}{(C_w + C_v + C_s)} \quad (5)$$

For the vegetation index calculated based on universal pattern decomposition method, universal pattern decomposition method (UPDM) standardized coefficients (371–2360 nm, the band interval of 1 nm) were first re-sampled to bandwidths of 5–35 nm, and then the vegetation canopy reflectance data obtained from PROSAIL model were simulated to 10–35 nm spectral reflectance data using a Gaussian spectral response function. The VIUPD index value was calculated from the standardized coefficients and reflectance data in the Interactive Data Language (IDL) program.

Many studies have focused on selecting the optimal characteristic band to construct spectral indices for LAI retrieval (Haboudane *et al.*, 2004; Wang *et al.*, 2005; Nguy-Robertson, 2013; Vuolo *et al.*, 2013). Because the reflectance spectral characteristics of the green vegetation canopy are mainly affected by the internal structure of the blade, the biochemical components of the blade and the canopy structure, there are differences in absorption and scattering properties of each biochemical component, and therefore different vegetation canopies have unique reflectances (Wang *et al.*, 2003; Sun and Cheng, 2010). According to the reflection spectral characteristics of carotenoid content, chlorophyll content, water content, nitrogen content and other components in plant leaves, six characteristic bands including 550 nm, 670 nm, 700 nm, 705 nm, 750 nm and 800 nm, which are sensitive for vegetation information were selected (Haboudane *et al.*, 2004; Delegido *et al.*, 2015). Additionally, based on the characteristic bands, seven spectral indices—normalized difference vegetation index (NDVI) (Lin and Liu, 2016), simple ratio indices (SRI), MSRI, TVI, modified soil adjusted vegetation indices (MSAVI), modified chlorophyll absorption reflectance indices (MCARI), and MCARI2 that are commonly and traditionally used for LAI retrieval, were selected (Table 3).

2.2.2 Sensitivity analysis

In order to quantitatively describe the sensitivity of spectral indices to LAI, the degree of change of SI with

Table 3 Selected spectral index for LAI retrieval

Spectral index	Formula
NDVI	$NDVI = (R_{750} - R_{705})/(R_{750} + R_{705})$
SRI	$SRI = R_{750}/R_{705}$
MSRI	$MSRI = (R_{750}/R_{705} - 1)/\sqrt{(R_{750}/R_{705} + 1)}$
TVI	$TVI = 0.5 \times [120 \times (R_{750} - R_{550}) - 200 \times (R_{670} - R_{550})]$
MSAVI	$MSAVI = 0.5[2R_{800} + 1 - \sqrt{(2R_{800} + 1)^2 - 8(R_{800} - R_{670})}]$
MCARI	$MCARI = [(R_{700} - R_{670}) - 0.2(R_{700} - R_{550})](R_{700}/R_{670})$
MCARI2	$MCARI2 = \frac{1.5[2.5(R_{800} - R_{670}) - 1.3(R_{800} - R_{550})]}{\sqrt{(2R_{800} + 1)^2 - (6R_{800} - 5\sqrt{R_{670}}) - 0.5}}$
VIUPD	$VIUPD = (C_v - 0.1 \times C_s - C_4)/(C_w + C_v + C_s)$

Notes: R_{550}, R_{670}, R_{700}, R_{705}, R_{750}, R_{800} represent reflectance at band 550 nm, 670 nm, 700 nm, 705 nm, 750 nm and 800 nm, respectively; C_w, C_v, C_s and C_4 are decomposition coefficients

changing LAI values was calculated according to Formula (6), and the definition of the sensitivity coefficient is as follows:

$$Var = \frac{(SI_{\max} - SI_{\min})}{SI_{\max}} \times 100\% \quad (6)$$

where SI represents the spectral index in the calculation, and $SI_{\max}$ and $SI_{\min}$ represent the maximum and minimum values of changes of this index along with variation of C_{a+b}, respectively. The degree of change in SI with variation in LAI was calculated based on Formula (5), and were defined as sensitivity coefficients.

2.2.3 Analysis of spectral scale effect

The value of spectral indices was not only related to changes in LAI, but was also affected by bandwidth, and degree of impact of bandwidth on different indices was different. The coefficient of variation was defined according to Formula (7) and simulated spectral index values at the bandwidths of 10 nm, 15 nm, 20 nm, 25 nm, 30 nm and 35 nm were compared to 5 nm as the reference in order to quantitatively compare and evaluate the magnitude of the effect of bandwidth on LAI.

$$Var = \frac{\left|(SI_{i,j} - SI_{5,j})\right|_{\max}}{(SI_5)_{\max}} \times 100\% \quad (7)$$

where i is bandwidth of 10, 15, 20, 25, 30, and 35 nm. j is LAI value, which ranges from 0.01 to 7.00. ($SI_{i,j}$ – $SI_{5,j}$) represents the difference between the spectral index value at the bandwidth of i and 5 nm under LAI value j.

3 Results

3.1 Correlation between spectral index and LAI

The eight selected spectral indices in this paper were calculated based on the reflectance data of seven bandwidths in the range of 5–35 nm, and the correlation between the spectral indices and LAI was first investigated. Figure 3 presents the variation of spectral indices under multiple bandwidths with increasing LAI value.

Eight spectral indices were overall logarithmically related to LAI (Fig. 3). In the mid-low LAI (LAI < 3.00) range, the spectral index value increased gradually with a gradual increase of LAI expect MCARI2; when LAI was greater than 3, spectral index values showed a trend of saturation, indicating that the spectral index methods selected in this paper are more suitable for the retrieval of LAIs with a middle to low value. Among them, the logarithmic correlation between MSAVI and MCARI2 was not obvious, and even started to show a trend of saturation in the range of LAI < 1. The coefficient of determination (R^2) between the spectral indices under multiple bandwidths and LAI are presented in Table 4.

At the canopy scale, the coefficients of determination of indices NDVI, SRI, MSRI, TVI, MCARI and VIUPD were greater than 0.5300, suggesting a good correlation with LAI. The R^2 for MSAVI and LAI was lower than 0.2000, showing a poor correlation; the R^2 for MCARI2 was 0.0152, indicating that there was nearly no correlation between MCARI2 and LAI.

3.2 Sensitivity analysis

The sensitivity coefficients for eight spectral indices with LAI variation are shown in Table 5. When LAI increased from 0.01 to 7.00, the sensitivities of the spectral indices calculated with seven bandwidths to the variation of LAI ranged from 69% to 71%, and the average change for the eight spectral indices was 70%.

Given that the spectral indices of NDVI, SRI, MSRI, TVI, MCARI and VIUPD all had a good correlation with LAI (Table 4), the index that exhibited a greater degree of change along with variation in LAI had a better sensitivity, and can better describe changes in LAI. Indices TVI and MCARI had the highest degrees of average change (99.30% and 99.49%, respectively),

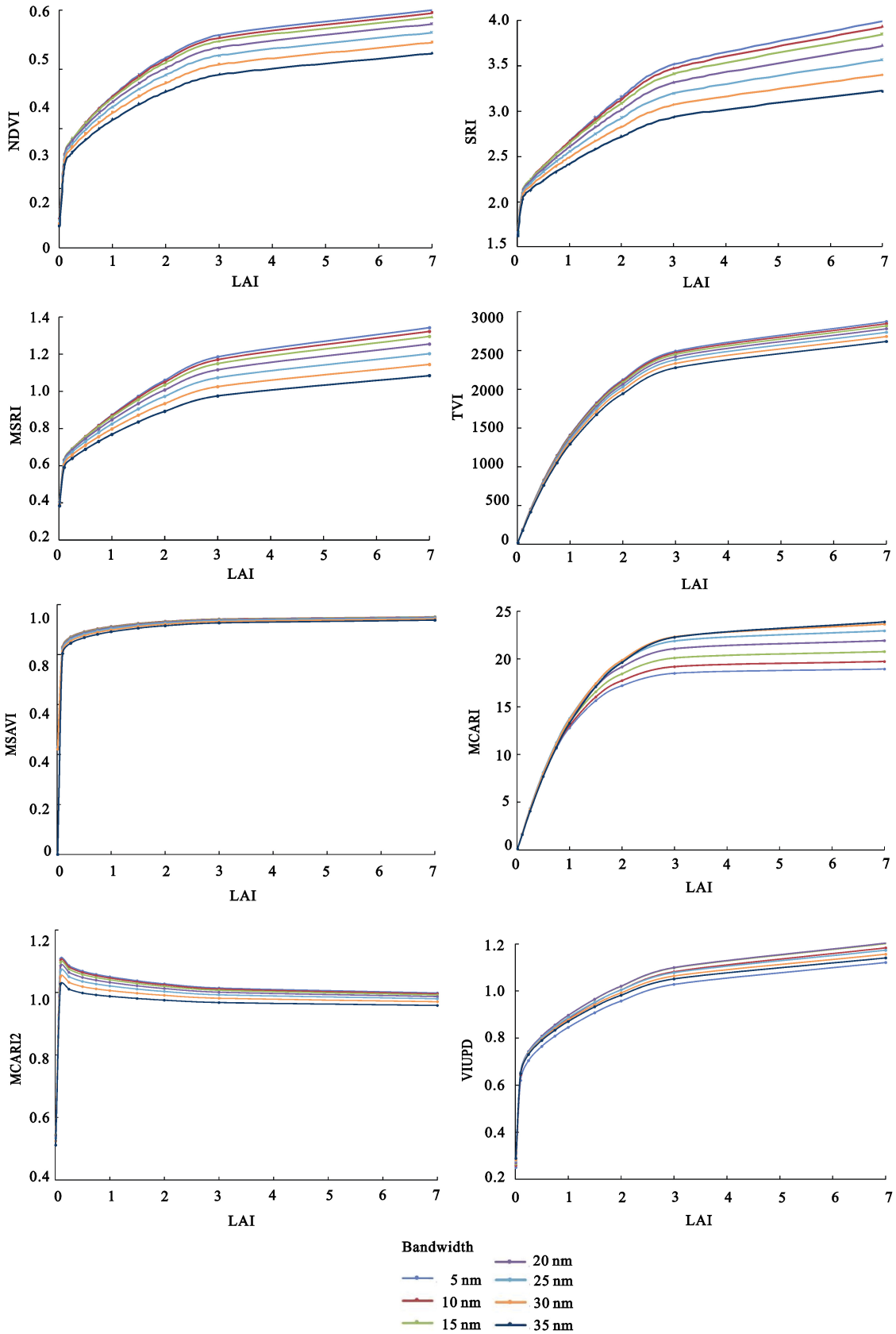

Fig. 3 Trends of spectral indices under seven bandwidths with increasing LAI

Table 4 Coefficient of determination (R^2) between spectral indices and LAI under multiple bandwidths

Spectral index	5 nm	10 nm	15 nm	20 nm	25 nm	30 nm	35 nm	Average
NDVI	0.6560	0.6492	0.6442	0.6394	0.6345	0.6293	0.6235	0.6395
SRI	0.8157	0.8088	0.8021	0.7937	0.7837	0.7722	0.7595	0.7908
MSRI	0.7525	0.7453	0.7389	0.7314	0.7228	0.7132	0.7026	0.7295
TVI	0.7212	0.7200	0.7191	0.7183	0.7179	0.7179	0.7185	0.7190
MSAVI	0.1760	0.1767	0.1784	0.1812	0.1852	0.1906	0.1972	0.1836
MCARI	0.5460	0.5586	0.5719	0.5883	0.6068	0.6264	0.6456	0.5919
MCARI2	0.0099	0.0105	0.0113	0.0130	0.0159	0.0201	0.0259	0.0152
VIUPD	0.5288	0.5396	0.5426	0.5463	0.5350	0.5329	0.5298	0.5364
Average	0.5258	0.5261	0.5261	0.5265	0.5252	0.5253	0.5254	0.5258

Table 5 Sensitivity coefficient of spectral indices under different bandwidths with LAI variation

Spectral index	5 nm	10 nm	15 nm	20 nm	25 nm	30 nm	35 nm	Average
NDVI	0.5850	0.5823	0.5774	0.5716	0.5651	0.5581	0.5509	0.5701
SRI	0.5843	0.5780	0.5689	0.5554	0.5385	0.5191	0.4982	0.5489
MSRI	0.6972	0.6933	0.6871	0.6788	0.6690	0.6580	0.6465	0.6757
TVI	0.9931	0.9931	0.9930	0.9930	0.9929	0.9929	0.9930	0.9930
MSAVI	0.5523	0.5504	0.5492	0.5492	0.5504	0.5525	0.5554	0.5513
MCARI	0.9944	0.9946	0.9947	0.9949	0.9951	0.9952	0.9953	0.9949
MCARI2	0.5081	0.5064	0.5036	0.5017	0.5010	0.5012	0.5021	0.5035
VIUPD	0.7768	0.7816	0.7791	0.7752	0.7624	0.7561	0.7471	0.7683
Average	0.7114	0.7099	0.7066	0.7025	0.6968	0.6917	0.6861	0.7007

and were the most sensitive to changes in LAI, followed by VIUPD and MSRI, which exhibited average changes of 76.83% and 67.57%, respectively, and also had a relatively good sensitivity to changes in LAI. The changes of the indices NDVI, SRI, MSAVI and MCARI2 were all less than 60%. In summary, the indices MSRI, TVI, MCARI and VIUPD displayed a relatively good performance in aspects of the correlation with LAI and the sensitivity to change in LAI.

3.3 Spectral scale effect

The coefficients of variation of the indices were in the ascending order of MSAVI, MCARI2, TVI, VIUPD, NDVI, MSRI, SRI, and MCARI (Table 6). The highest coefficients of variation were found in indices MSRI, SRI and MCARI (> 9.3) while the remaining indices were less than 6%. The spectral indices calculated at bandwidths of 10 nm, 15 nm, 20 nm, 25 nm, 30 nm, and 35 nm were compared to indices at 5 nm, and average changes were 1.9%, 3.7%, 5.8%, 7.8%, 10.1% and 12.4%, respectively. The most significant difference occurred between the spectral index calculated at a bandwidth of 35 nm and 5 nm. Overall, when the bandwidth increased from 5 nm to 35 nm, the average coefficient of variation of all spectral indices were 6.9%.

In the above studies, the spectral indices that had a high correlation with LAI, that were sensitive to changes in LAI and that were less affected by changes in bandwidth had the best retrieval performance. In terms of correlation with LAI, except for indices MSAVI and MCARI2 those had coefficients of determination lower than 0.2 and exhibited a poor correlation, other indices had coefficients of determination

Table 6 Coefficient of variation of spectral indices with bandwidth variation

Spectral index	10 nm	15 nm	20 nm	25 nm	30 nm	35 nm	Average
NDVI	0.0087	0.0204	0.0388	0.0629	0.0910	0.1216	0.0572
SRI	0.0160	0.0371	0.0688	0.1078	0.1501	0.1929	0.0954
MSRI	0.0150	0.0350	0.0657	0.1042	0.1473	0.1922	0.0932
TVI	0.0091	0.0190	0.0319	0.0478	0.0669	0.0890	0.0439
MSAVI	0.0018	0.0026	0.0056	0.0108	0.0184	0.0281	0.0112
MCARI	0.0416	0.0961	0.1567	0.2114	0.2481	0.2604	0.1691
MACRI2	0.0044	0.0106	0.0202	0.0337	0.0514	0.0730	0.0322
VIUPD	0.0555	0.0713	0.0735	0.0466	0.0318	0.0341	0.0521
Average	0.0190	0.0365	0.0577	0.0781	0.1006	0.1239	0.0693

higher than 0.53. The coefficients of variation of indices TVI, MCARI, VIUPD and MSRI derived from the changes of LAI were more than 67%, and the changes of NDVI, SRI, MSAVI and MCARI2 were less than 60% but more than 50%, indicating that the selected eight indices all possessed relatively good sensitivity to changes in LAI. In the study on the sensitivity to the bandwidth variations, the coefficients of variation of indices MSAVI, MCARI2, TVI, VIUPD and NDVI derived from the bandwidth variations were all less than 6%, i.e., a relatively small uncertainty of the spectral scale.

Taken together, spectral decomposition mode-based VIUPD, NDVI combined with red edge position information, and TVI were less impacted by spectral scale and had better LAI retrieval capabilities.

4 Discussion

4.1 Establishment of model for LAI retrieval

An appropriate regression model was established using the above simulated spectral index values with seven bandwidths and corresponding LAIs. In this study, there were 70 samples of spectral indices and LAI with ten leaf area levels and seven bandwidths. After the regression model was built, root mean squared error (RMSE) was used to evaluate the predictive ability of the model, and to test and analyze the agreement between simulated and measured values.

Performances of SIs were evaluated by comparing the variation in coefficient of determination (R^2) and root mean squared error (RMSE) (Wu *et al*., 2010). Higher R^2 and lower RMSE would have higher accuracy and precision of a given SI to estimate LAI.

The indices VIUPD and NDVI had the best regression relationship with LAI ($R^2 > 0.97$, RMSE < 0.9); R^2 values of the regression equations established from indices MSRI, TVI, MSAVI and MCARI were all more than 0.85, and RMSE values were less than 1.35 (Table 7). Although the regression coefficient of index SRI was more than 0.9, the corresponding RMSE was the largest, i.e., there was a poor retrieval accuracy. MCARI2 failed to exhibit a strong relationship with LAI ($R^2 < 0.45$, RMSE > 2.2).

4.2 Validation of spectral scale effect during LAI retrieval

The 5 nm canopy reflectance data got from the PROSAIL model, which was used to simulate reflectance data at bandwidths of 40 nm, 45 nm, 50 nm, 55 nm, 60 nm and 65 nm; eight spectral indices under each bandwidth were calculated and LAI was retrieved based on the established regression model.

Table 7 Spectral indices and regression models for LAI

Spectral index	Regression model	R^2	RMSE
NDVI	$y = 434.92x^{7.5999}$	0.9703	0.8077
SRI	$y = 0.0005x^{7.6596}$	0.9191	2.5926
MSRI	$y = 2.2284x^{5.6635}$	0.9630	1.3306
TVI	$y = 0.0002x^{1.2132}$	0.9632	1.1251
MSAVI	$y = 0.00006e^{10.867x}$	0.7963	1.7474
MCARI	$y = 0.0467e^{0.2193x}$	0.8613	1.0987
MCARI2	$y = 0.7602x^{6.0286}$	0.4459	2.2156
VIUPD	$y = 0.0013e^{7.3911x}$	0.9855	0.5914

Finally, the retrieved LAI values were fitted to the actual values. And the actual LAI got from the input parameters of the PROSAIL model, i.e., 0.01 to 7.00. Figure 4 displays the fitting situation of retrieved LAI values and actual values based on spectral index method.

The best degree of fit was found between the retrieved LAI values from index VIUPD; the regression line was close to 1∶1 line, the R^2 value was 0.9884, and the retrieved values were in the range of 0–6, which were closest to actual values (Fig. 4). Followed by VIUPD, indices MCARI and TVI showed the second performance, with R^2 being more than 0.75. The range of the retrieved value for MCARI was from 0 to 9, slightly higher than the actual value, while the retrieved value of TVI was between 0 and 3.5, lower than the actual value. The R^2 values of NDVI, SRI, MSRI and MSAVI were greater than 0.6, but ranges of the retrieved values were also lower than the actual value. The retrieved values of MSAVI ranged only between 0 and 1.6, and the retrieval results lacked validity. The retrieved LAI values based on the index MCARI2 showed the worst degree of fit with the actual value, and were not suitable for the LAI retrieval at the canopy scale in this study.

4.3 Summary of performance of spectral index

The pattern decomposition method (PDM) was first used to study Landsat Multispectral Scanner (MSS) and Thematic Mapper (TM) satellite remote sensing data, and is a hybrid linear spectral model. In order to overcome

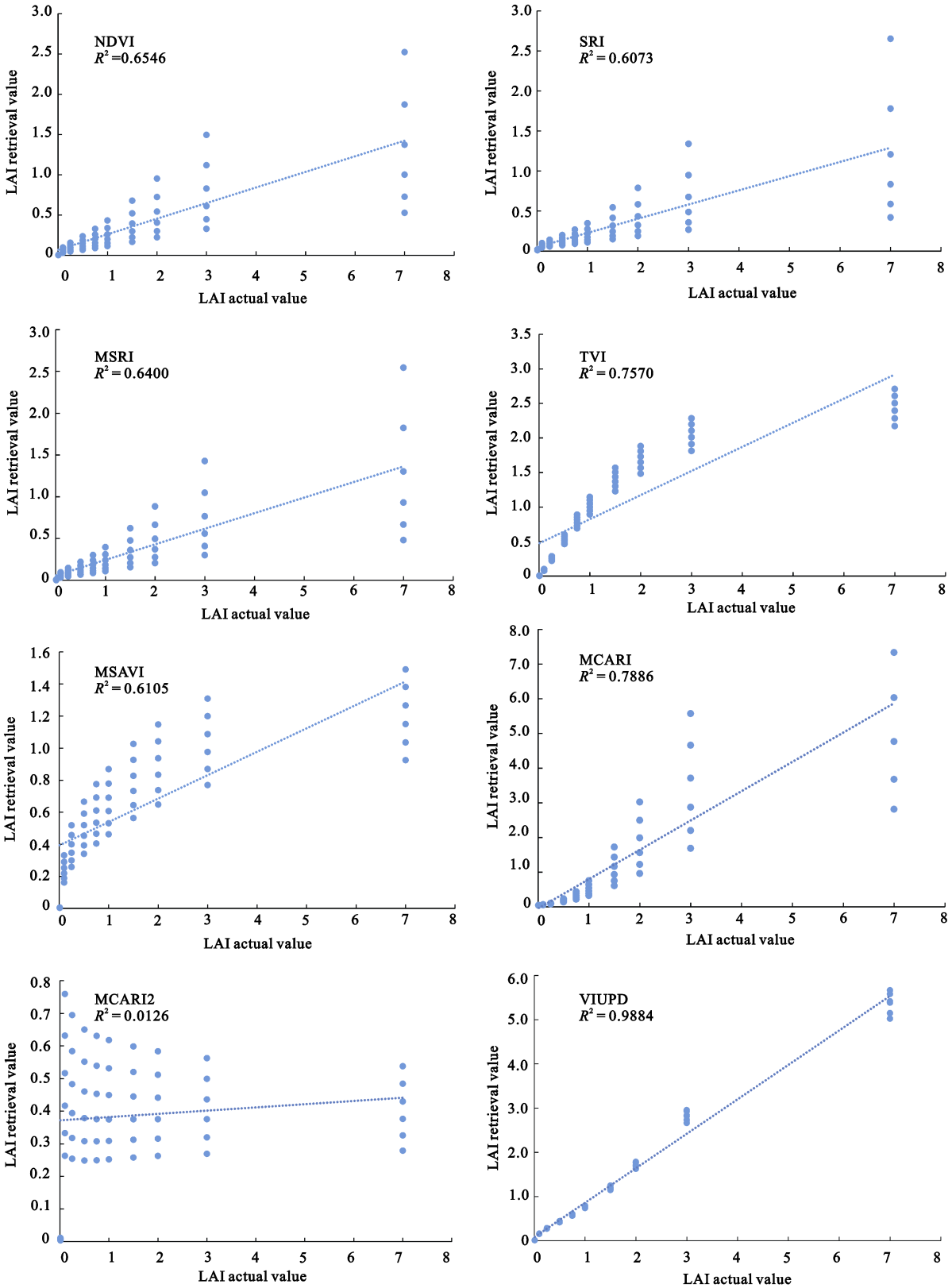

Fig. 4 Degree of fit between retrieved value and actual value of LAI

limitations of PDM, the spectral data of continuous ground objects is normalized in UPDM, which has a coefficient that is characterized as ″independent from the sensor″. The VIUPD is a new spectral index based on UPDM, and also is ″not affect by the sensors″. In this study, VIUPD was well correlated with LAI, was not affected by changes in bandwidth, and showed a relatively good retrieval capability (Zhang *et al*., 2006). This conclusion validates the feature of VIUPD being ″independent of the sensor″ and also suggests that VIUPD meets the needs of applications using different multiple/ hyperspectral sensor data analysis while achieving accurate retrieval of multi-source remote sensing data, such as vegetation physicochemical parameters at different spatial scales. Therefore, the use of the spectral index VIUPD has broad prospects for application during estimation of LAI and even during retrieval of vegetation physiological and biochemical parameters.

Red edge position is the wavelength position corresponding to the maximum value of the first order differential of the vegetation reflectance spectra, and is usually located between 650 and 750 nm (Kim and Yeom, 2014; Li *et al.*, 2014). The shift of red edge position to a longer wavelength reflects an increase in chlorophyll content of plant leaves, and red edge position will move to a shorter wavelength when chlorophyll content is reduced (Filella, 1994: Danson and Plummer, 1995). In this study, the red edge position information was incorporated during the construction of the indices NDVI, SRI and MSRI, and relatively good retrieval results were obtained, supporting the hypothesis that vegetation red edge position can be used to describe changes in chlorophyll content and canopy LAI. Although the accuracy of LAI retrieval using SRI and MSRI was high, the spectral scale effects were really impacted by changes in bandwidth.

MCARI is a variation of chlorophyll absorption reflectance indices (CARI). The introduction of R_{700}/R_{670} can minimize the effect of soil reflectance but sensitivity to background reflectance properties still remains (Nguy-Robertson, 2013). In this paper, the LAI-retrieval accuracies of MCARI and MCARI2 were low and the spectral scale effect was significant, perhaps due to the interference from the soil background. Daughtry (2000) proposed combining MCARI with optimized soil adjusted vegetation index (OSAVI) to reduce the contribution of background emission rate from background soil and to enhance the sensitivity of physiological and biochemical vegetation parameters (Daughtry *et al*., 2000). Therefore, further research can attempts to combine OSAVI and traditional forms of spectral indices that are sensitive to vegetation biochemical parameters in order to study the spectral scale effect during canopy LAI retrieval using spectral indices after the soil background effect has been weakened.

The correlation of spectral indices with LAI, the sensitivity of spectral indices to changes in LAI, and the sensitivity of spectral indices to the changes of bandwidth were studied here. The spectral decomposition mode-based VIUPD, NDVI combined with red edge position information, and TVI had better performance for LAI retrieval and were less impacted by spectral scale. This was consistent with results of the validation of the sensitivities of these spectral indices to bandwidth. VIUPD had the best retrieval accuracy, followed by NDVI and TVI, which had retrieval accuracies higher than those of other indices.

5 Conclusions

Based on the vegetation radiative transfer model, the spectral scale effect generated from LAI retrieval using the spectral index model method was studied in this paper. The coupled leaf-canopy-PROSAIL model was used to simulate canopy spectral reflectance data at bandwidth of 5 nm under different LAI levels (0.01–7.00), and the Gaussian spectral response function was used to simulate reflectance data at bandwidths of 10 nm, 15 nm, 20 nm, 25 nm, 30 nm and 35 nm. Subsequently, eight spectral indices (NDVI, SRI, MSRI, TVI, MSAVI, MCARI, MCARI2 and VIUPD) using seven bandwidths were evaluated in terms of correlation with LAI, sensitivity to changes of LAI, and sensitivity to changes in bandwidth. The results showed that the spectral decomposition mode-based VIUPD, NDVI combined with red edge position information, and TVI showed better performance for LAI retrieval. Results on the sensitivity of spectral indices to changes of bandwidth were validated using simulated canopy reflectance data at bandwidths of 40 nm, 45 nm, 50 nm, 55 nm, 60 nm and 65 nm. In conclusion, the spectral index VIUPD showed the highest retrieval accuracy and

the best degree of fit between retrieved values and actual values. NDVI and TVI exhibited the second performance with coefficients of determination R^2 more than 0.96, though retrieved values were less than actual values. The retrieval results of the remaining indices were poor. In summary, when the spectral index method is used to retrieve LAI based on multiple sensor data, due to differences in sensor spectral response (bandwidth and center wavelength), the impact of spectral scale effect on retrieval results should be considered in order to provide a better synergistic retrieval of LAI and other vegetation physiological and biochemical parameters using multi-source remote sensing data.

The red edge position information was incorporated into NDVI and a relatively good LAI-retrieval result was obtained, providing support to the hypothesis that vegetation red edge position can be used to describe changes in LAI. The principle used to construct TVI was to use the area of the triangle formed from the reflectance at 550 nm, 670 nm and 750 nm (Bannari *et al.*, 1995). In TVI, two important spectral characteristics, vegetation red absorption trough and near infrared reflectance peak, were taken into account. When the reflectance for red light decreased and reflectance of near-infrared light increased, the area of the triangle increased, which could partially eliminate impacts of the atmospheric environment, solar elevation angle, and the viewing angle of remote sensing sensors. These factors play a decisive role in obtaining a relatively good LAI retrieval accuracy.

The spectral scale effect during vegetation LAI retrieval with using spectral indices was investigated. Some studies have explored retrieval accuracy and spatial scale effect during retrieval of vegetation biochemical parameters under different spatial scales (terrestrial, aerial and satellites). In the present paper, differences in spectral scale effect during the retrieval of LAI or other biochemical parameters under different spatial scales as well as corresponding causes were explored. The data used in this paper were the canopy reflectance spectral data simulated from the vegetation radiative transfer model and multi-band spectral data simulated from the Gaussian spectral response model. Although the spectral scale effects were confirmed, spectral data with relatively significant differences in synchronous spectral resolution from the measurement should be collected in order to test the validity of the spectral scale effect generated during LAI retrieval.

References

Bannari A, Morin D, Bonn F *et al.*, 1995. A review of vegetation indices. *Remote Sensing Reviews*, 13(1): 95–120. doi: 10.1080/02757259509532298

Bicheron P, Leroy M, 1999. A method of biophysical parameter retrieval at global scale by inversion of a vegetation reflectance model. *Remote Sensing of Environment*, 67(3): 251–266. doi: 10.1016/S0034-4257(98)00083-2

Broge N H, Leblanc E, 2001. Comparing prediction power and stability of broadband and hyperspectral vegetation indices for estimation of green leaf area index and canopy chlorophyll density. *Geochimica Et Cosmochimica Acta*, 76(2): 156–172. doi: 10.1016/S0034-4257(00)00197-8

Cho M A, Skidmore A K, 2006. A new technique for extracting the red edge position from hyperspectral data: the linear extrapolation method. *Remote Sensing of Environment*, 101(2): 181–193. doi: 10.1016/j.rse.2005.12.011

Danson F M, Plummer S E, 1995. Red-edge response to forest leaf area index. *International Journal of Remote Sensing*, 16(1): 183–188. doi: 10.1080/01431169508954387

Darvishzadeh R, Skidmore A, Schlerf M *et al.*, 2008a. Inversion of a radiative transfer model for estimating vegetation LAI and chlorophyll in a heterogeneous grassland. *Remote Sensing of Environment*, 112(5): 2592–2604. doi: 10.1016/j.rse.2007.12.003

Darvishzadeh R, Skidmore A, Schlerf M *et al.*, 2008 b. LAI and chlorophyll estimation for a heterogeneous grassland using hyperspectral measurements. *Isprs Journal of Photogrammetry & Remote Sensing*, 63(4): 409–426. Doi: 10.1016/j.isprsjprs.2008.01.001

Daughtry C S T, Walthall C L, Kim M S *et al.*, 2000. Estimating corn leaf chlorophyll concentration from leaf and canopy reflectance. *Remote Sensing of Environment*, 74(2): 229–239. doi: 10.1016/S0034-4257(00)00113-9

Delegido J, Verrelst J, Rivera J P *et al.*, 2015. Brown and green, lai mapping through spectral indices. *International Journal of Applied Earth Observation & Geoinformation*, 35(Part B): 350–358. doi: 10.1016/j.jag.2014.10.001

Elvidge C D, Chen Z, 1995. Comparison of broad-band and narrow-band red and near-infrared vegetation indices. *Remote Sensing of Environment*, 54(1): 38–48. doi: 10.1016/0034-4257(95)00132-K

Everitt J H, Yang C, 2007. Mapping broom snakeweed through image analysis of color-infrared photography and digital imagery. *Environmental Monitoring & Assessment*, 134(1–3): 287–92. doi: 10.1007/s10661-007-9619-0

Feret J B, François C, Asner G P *et al.*, 2008. Prospect-4 and 5: advances in the leaf optical properties model separating photosynthetic pigments. *Remote Sensing of Environment*, 112(6): 3030–3043. doi: 10.1016/j.rse.2008.02.012

Filella I, 1994. The red edge position and shape as indicators of plant chlorophyll content, biomass and hydric status. *Interna-*

tional Journal of Remote Sensing, 15(7): 1459–1470. doi: 10.1080/01431169408954177

Goel N S, Thompson R L, 1984. Inversion of vegetation canopy reflectance models for estimating agronomic variables. v. estimation of leaf area index and average leaf angle using measured canopy reflectances. *Remote Sensing of Environment*, 16(1): 69–85. doi: 10.1016/0034-4257(84) 90028-2

Haboudane D, Miller J R, Pattey E *et al.*, 2004. Hyperspectral vegetation indices and novel algorithms for predicting green lai of crop canopies: modeling and validation in the context of precision agriculture. *Remote Sensing of Environment*, 90(3): 337–352. doi: 10.1016/j.rse.2003.12.013

Haboudane D, Miller J R, Tremblay N *et al*., 2002. Integrated narrow-band vegetation indices for prediction of crop chlorophyll content for application to precision agriculture. *Remote Sensing of Environment*, 81(2–3): 416–426. doi: 10. 1016/S0034-4257(02)00018-4

Houborg R, Soegaard H, Boegh E, 2007. Combining vegetation index and model inversion methods for the extraction of key vegetation biophysical parameters using terra and aqua modis reflectance data. *Remote Sensing of Environment*, 106(1): 39–58. doi: 10.1016/j.rse.2006.07.016

Jacquemoud S, Baret F, 1990. PROSPECT: a model of leaf optical properties spectra. *Remote sensing of Environment*, 34(2): 75–91. doi: 10.1016/0034-4257(90)90100-Z

Jacquemoud S, Baret F, Andrieu B *et al.*, 1995. Extraction of vegetation biophysical parameters by inversion of the prospect + sail models on sugar beet canopy reflectance data: application to tm and aviris sensors. *Remote Sensing of Environment*, 52(3): 163–172. doi: 10.1016/0034-4257(95)00018-V

Kim H O, Yeom J M, 2014. Effect of red-edge and texture features for object-based paddy rice crop classification using rapideye multi-spectral satellite image data. *International Journal of Remote Sensing*, 35(19): 7046–7068. doi: 10.1080/01431161.2014.965285

Li F, Miao Y X, Feng G H *et al.*, 2014. Improving estimation of summer maize nitrogen status with red edge-based spectral vegetation indices. *Field Crops Research*, 157(2): 111–123. doi: 10.1016/j.fcr.2013.12.018

Lin Sen, Liu Ronggao, 2016. A simple method to extract tropical monsoon forests using NDVI based on MODIS data: a case study in South Asia and Peninsula Southeast Asia. *Chinese Geographical Science*, 26(1): 22–34. doi: 10.1007/s11769-015-0789-3

Marceau D J, Hay G J, 1999. Remote sensing contributions to the scale issue. *Canadian Journal of Remote Sensing Journal Canadien De Télédétection*, 25(4): 357–366. doi: 10.1080/07038992.1999.10874735

Moody A, Woodcock C E, 1995. The influence of scale and the spatial characteristics of landscapes on land-cover mapping using remote sensing. *Landscape Ecology*, 10(6): 363–379. doi: 10.1007/BF00130213

Nguy-Robertson A L, 2013. The mathematical identity of two vegetation indices: mcari2 and mtvi2. *International Journal of Remote Sensing*, 34(34): 7504–7507. doi: 10.1080/01431161.2013.823525

Paul J C, Edward J M, 1983. The relationships between the chlorophyll concentration, LAI and reflectance of a simple vegetation canopy. *International Journal of Remote Sensing*, 4(2): 247–255. doi: 10.1080/01431168308948544

Pisek J, Chen J M, 2007. Comparison and validation of modis and vegetation global LAI products over four bigfoot sites in north America. *Remote Sensing of Environment*, 109(1): 81–94. doi: 10.1016/j.rse.2006.12.004

Rogers J N, Parrish C E, Ward L G *et al.*, 2015. Evaluation of field-measured vertical obscuration and full waveform lidar to assess salt marsh vegetation biophysical parameters. *Remote Sensing of Environment*, 156: 264–275. doi: 10.1016/j.rse.2014.09.035

Stéphane J, Wout V, Frédéric B *et al.*, 2009. Prospect + sail models: a review of use for vegetation characterization. *Remote Sensing of Environment*, 113(2009): S56–S66. doi: 10. 1016/j.rse.2008.01.026

Su Lihong, Li Xiaowen, Huang Yuxia, 2001. A review on scale in remote sensing. *Advance in Earth Sciences*, 16(4): 544–548. (in Chinese)

Sun Li, Cheng Lijuan, 2010. Analysis of spectral response of vegetation leaf biochemical components. *Spectroscopy & Spectral Analysis*, 30(11): 3031–3035(5). (in Chinese)

Teillet P M, Staenz K, William D J, 1997. Effects of spectral, spatial, and radiometric characteristics on remote sensing vegetation indices of forested regions. *Remote Sensing of Environment*, 61(1): 139–149. doi: 10.1016/S0034-4257(96)00248-9

Thenkabail P S, Smith R B, Pauw E D, 2000. Hyperspectral vegetation indices and their relationships with agricultural crop characteristics. *Remote Sensing of Environment*, 71(2): 158–182. doi: 10.1016/S0034-4257(99)00067-X

Vuolo F, Neugebauer N, Bolognesi S F *et al.*, 2013. Estimation of leaf area index using deimos-1 data: application and transferability of a semi-empirical relationship between two agricultural areas. *Remote Sensing*, 5(3): 1274–1291. doi: 10.3390/rs5031274

Weiss M, Baret F, Smith G J, 2004. Review of methods for in situ leaf area index (LAI) determination: part ii. estimation of LAI, errors and sampling. *Agricultural & Forest Meteorology*, 121(1): 37–53. doi: 10.1016/j.agrformet.2003.08.001

Wu C Y, Han X Z, Niu Z*et al.,* 2010a. An evaluation of eo-1 hyperspectral hyperion data for chlorophyll content and leaf area index estimation. *International Journal of Remote Sensing*, 31(4): 1079–1086. doi: 10.1080/01431160903252335

Wu C Y, Niu Z, Wang J D *et al.*, 2010b. Predicting leaf area index in wheat using angular vegetation indices derived from in situ canopy measurements. *Canadian Journal of Remote Sensing*, 36(4): 301–312. doi: 10.5589/m10-050

Wang Jihua, Huang Wenjiang, Zhao Chunjiang *et al.*, 2003. The inversion of leaf biochemical components and grain quality indicators of winter wheat with spectral reflectance. *Journal of Remote Sensing*, (4): 277–284. (in Chinese)

Wang Q, Samuel A, John T *et al.*, 2005. On the relationship of ndvi with leaf area index in a deciduous forest site. *Remote*

Sensing of Environment, 94(2): 244–255. doi: 10.1016/j.rse.2004.10.006

Wen J G, Liu Q, Liu Q H *et al.*, 2009. Scale effect and scale correction of land-surface albedo in rugged terrain. *International Journal of Remote Sensing*, 30(20): 5397–5420. doi: 10.1080/01431160903130903

Zhang L F, Furumi S, Muramatsu K *et al.*, 2006. Sensor- independent analysis method for hyperspectral data based on the pattern decomposition method. *International Journal of Remote Sensing*, 27(21): 4899–4910. doi: 10.1080/01431160600702640

Zhang L F, Furumi S, Muramatsu K *et al.*, 2007. A new vegetation index based on the universal pattern decomposition method. *International Journal of Remote Sensing*, 28(1–2): 107–124. doi: 10.1080/01431160600857402

Zhang L F, Liu B, Zhang B*et al.*, 2010. An evaluation of the effect of the spectral response function of satellite sensors on the precision of the universal pattern decomposition method. *International Journal of Remote Sensing*, 31(8): 2083–2090. doi: 10.1080/01431160903246675